

Pressure sources versus surface loads: Analyzing volcano deformation signal composition with an application to Hekla volcano, Iceland

Ronni Grapenthin,¹ Benedikt G. Ófeigsson,² Freysteinn Sigmundsson,² Erik Sturkell,³ and Andrew Hooper⁴

Received 5 July 2010; revised 10 September 2010; accepted 15 September 2010; published 26 October 2010.

[1] The load of lava emplaced over periods of decades to centuries induces a gradual viscous response of the Earth resulting in measurable deformation. This effect should be considered in source model inversions for volcanic areas with large lava production and flow emplacement in small centralized regions. If deformation data remain uncorrected, constructive load and pressure source interference may result in an overestimate of depth and volume of a magma reservoir whereas destructive signal interference may cause these values to be underestimated. In both cases the source geometry preference could be biased. The ratio of horizontal and vertical displacements aids the identification of composite signals. We provide a method to quantify and remove the lava load deformation signals, using deformation at Hekla volcano, Iceland as an example.

Citation: Grapenthin, R., B. G. Ófeigsson, F. Sigmundsson, E. Sturkell, and A. Hooper (2010), Pressure sources versus surface loads: Analyzing volcano deformation signal composition with an application to Hekla volcano, Iceland, *Geophys. Res. Lett.*, 37, L20310, doi:10.1029/2010GL044590.

1. Introduction

[2] Deformation of the Earth's surface provides critical information about magma migration beneath a volcano. The respective displacements, recorded by geodetic techniques such as GPS or InSAR, are commonly inverted for parameters that describe the plumbing system of volcanoes. Evaluation of such modeling efforts often focuses on model validity and assumptions with regard to crustal composition, such as the level of inhomogeneity, elastic versus plastic deformation, thermal effects, or the compressibility of materials [e.g., *Masterlark*, 2007]. While effects of topography [*McTigue and Segall*, 1988; *Williams and Wadge*, 2000], magma compressibility [e.g., *Rivalta and Segall*, 2008], and viscoelastic media [*Bonafede and Ferrari*, 2009] on deformation due to buried sources have been explored, correcting deformation signals for surface load contribution prior to source inversions seems to remain largely neglected.

[3] Surface loads contribute to deformation in various ways, including mass variations of ice caps and glaciers [e.g., *Pagli and Sigmundsson*, 2008], seasonal load variations [e.g., *Heki*, 2001; *Grapenthin et al.*, 2006], elastic response to lava flows [e.g., *Lu et al.*, 2003], or volcanic edifice destruction [e.g., *Pinel and Jaupart*, 2005]. These can induce significant deformation which may result in changes of the productivity of a magmatic system [e.g., *McNutt and Beavan*, 1987; *Jull and McKenzie*, 1996; *Pinel and Jaupart*, 2005; *Pagli and Sigmundsson*, 2008].

[4] Post-eruptive deformation due to lava flow loads involving a thin viscoelastic substrate to explain deformation in immediate surroundings of lava flows over time scales of several years has been previously suggested [e.g., *Briole et al.*, 1997]. Here we show, that a gradual viscous response to lava loads emplaced over periods of decades to centuries also needs to be considered in magma source inversions. At volcanoes with high lava production that deposit in comparably small areas (e.g., Hekla, Iceland), the viscous response to the load is expected to induce a displacement pattern with long wavelength characteristics similar to those of a deflating magma reservoir (Figure 1a). In such regions deformation originating from superposition of lava load and magma source signals is expected to be commonly observed. We demonstrate that such observations must be load corrected prior to any source inversion to retrieve reliable parameters. As a first order approach to identify such composite deformation signals we can employ the ratio of horizontal and vertical deformation [*Pinel et al.*, 2007], as vertical deformation is much more pronounced in surface loading. We apply this to observations at Hekla volcano and develop an algorithm to quantify and remove the load contribution from the deformation signal.

2. Pressure Source and Surface Load Models

[5] An internal pressure change in a spherical magma reservoir is often described as a pressure point source embedded in an elastic half-space [e.g., *Mogi*, 1958]. This "Mogi model" explains surface deformation with 4 parameters: horizontal coordinates of the source's center, depth and source strength. The depth determines whether the displacement is very localized (shallow source) or regionally distributed (deep source). The source strength (i.e., scaled volume change) controls the amplitude of the signal. In addition to the Mogi model we consider deformation due to a fully horizontal rectangular magma body (sill) which is modeled as a tensile fault as described by *Okada* [1992].

[6] To model surface load changes over long periods we consider both elastic and viscous responses. The emplacement of a load on the surface of an Earth in lithostatic

¹Geophysical Institute, University of Alaska Fairbanks, Fairbanks, Alaska, USA.

²Nordic Volcanological Center, Institute of Earth Sciences, University of Iceland, Reykjavík, Iceland.

³Department of Earth Sciences, University of Gothenburg, Gothenburg, Sweden.

⁴Delft Institute of Earth Observation and Space Systems, Delft University of Technology, Delft, The Netherlands.

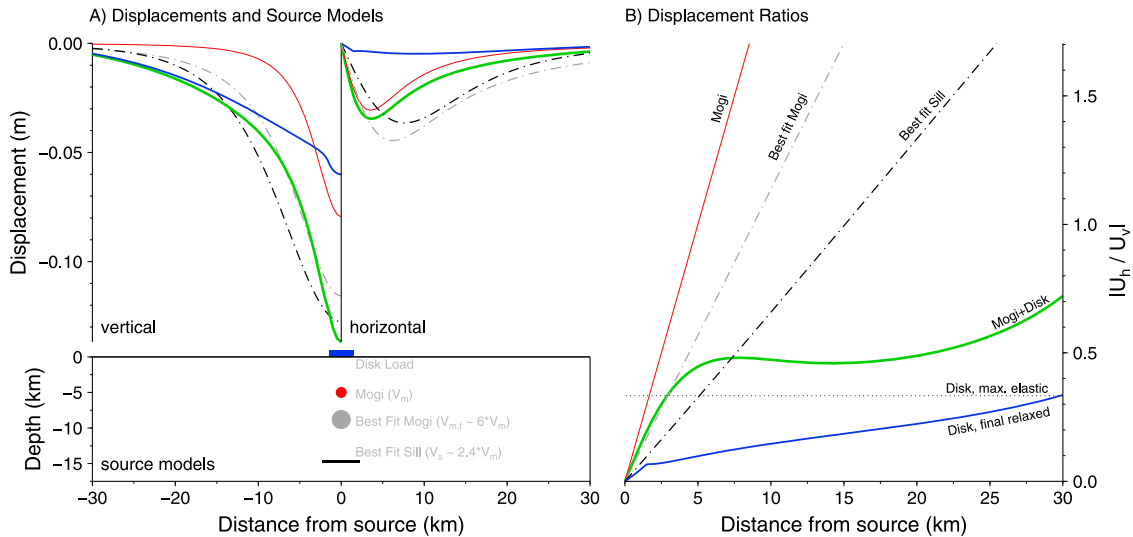


Figure 1. (a) Deformation source models at the bottom and respective vertical and horizontal displacements on top. (bottom) Earth model is elastic half-space for magmatic sources, but thick elastic plate over an inviscid fluid [Pinel *et al.*, 2007] for the surface load. Depth is not to scale to source sizes. Parameters for surface load model: elastic plate thickness, $H = 5$ km, Poisson's ratio, $\nu = 0.25$, effective Young's modulus, $E = 40$ GPa, viscous fluid density, $\rho_f = 3100$ kg m $^{-3}$. Disk load (blue) has density, radius, and uniform height of $\rho = 2700$ kg m $^{-3}$, $r = 1500$ m, $h = 7.5$ m, respectively. The forward modeled Mogi source (red) changes volume by $V = -0.025$ km 3 at $d = 5$ km depth. Grey circle and black line show the sources that fit the superimposed deformation of disk and Mogi source best. (top) Displacements due to the models described above, colors are labeled in Figure 1b and correspond to the respective sources in Figure 1a. The sum of disk and Mogi source is green. Inversions are dash-dotted. Note the large misfit in the horizontal for inverted sources due to the small contribution of the disk load in the horizontal deformation field. (b) Displacement ratios as a means to identify composite deformation signals, see text.

equilibrium induces an instantaneous elastic response in the lithosphere. For a load of arbitrary shape the respective displacements can be inferred by convolving the load with a Green's function that describes the elastic response to a point source of pressure [e.g., Grapenthin *et al.*, 2006; Pinel *et al.*, 2007]. Given sufficient duration and magnitude (or wavelength) of the load, a slow viscous response of ductile material in crust and mantle follows until after decades to centuries a new state of isostatic equilibrium, the final relaxed state, is reached. Similar to the elastic case, the response can be found using an appropriate Green's function. The transition from instantaneous to final relaxed response typically occurs with an exponential displacement rate as observed for post-glacial isostatic adjustment [e.g., Wu *et al.*, 1998]. To model this transition the use of a single effective relaxation time was suggested by Pinel *et al.* [2007] which results in deformation similar to a load on an elastic plate overlying a half-space of Newtonian viscosity. We model crustal responses to lava load changes on a flat Earth using Green's functions derived by Pinel *et al.* [2007] which are implemented in the software framework CrusDe [Grapenthin, 2007]. CrusDe's sources and the model files used in this study are published under the terms of the GNU Public License and freely available at <http://www.gps.alaska.edu/crusde>.

[7] A major pitfall in analyzing responses to surface loading and internal pressure change is the apparent resemblance of their deformation pattern. A combination of the crust's elastic layer and viscous creep of the ductile crust and mantle effectively turns the lithosphere into a time dependent low-pass filter (with Maxwell response time) for

deformation signals induced by loads. Hence, all the high-frequency (i.e., short wavelength) features of complex loads such as lava flows are lost in the respective deformation pattern. This results in a long wavelength deformation pattern similar to displacements caused by buried pressure sources (see Figure 1a). Given separated records for horizontal and vertical deformation, however, vertical deformation clearly dominates the surface load response. Therefore, we can employ the ratio $R_{h,z} = |U_h/U_z|$ of horizontal, U_h , and vertical, U_z , displacements to analyze the deformation signal [Pinel *et al.*, 2007]. For the Mogi point source and the simplified tensile fault model used here [Lisowski, 2007], $R_{h,z} = r/d$ is a linear function that depends on depth, d , and horizontal distance from the center of the source, r . Surface load deformation, on the contrary, results in a non-linear ratio (Figure 1b). Pinel *et al.* [2007] show for their elastic Green's functions (Poisson's ratio = 0.25) the ratio $R_{h,z}$ will never exceed $\frac{1}{3}$. The final relaxed ratio remains smaller than the elastic ratio until the vertical deformation approaches zero which results in a narrow spike in the far field.

3. Identification of Composite Deformation Signals

[8] We demonstrate the effect of a surface load on depth and volume estimates for a magmatic source by superimposing subsidence due to load emplacement on deflation of a hypothetical spherical magma reservoir that is approximated by a Mogi source. The inversions of the composite signal are then carried out for a magma reservoir only.

[9] Let us assume the application of a lava flow to a flat surface in form of a disk load with density $\rho = 2700 \text{ kg m}^{-3}$, radius $r = 1500 \text{ m}$, and uniform height $h = 7.5 \text{ m}$ (Figure 1a). The blue line in Figure 1a shows the vertical and horizontal final relaxed response. Deflation of a spherical magma reservoir at depth $d = 5 \text{ km}$ with a volume decrease $V = -0.025 \text{ km}^3$ results in subsidence shown by the red line in Figure 1a. The superposition of the two signals is represented by the green line in Figure 1a. At a first glance the displacement field of the superposed signal does indeed resemble the shape of displacements due to a Mogi source.

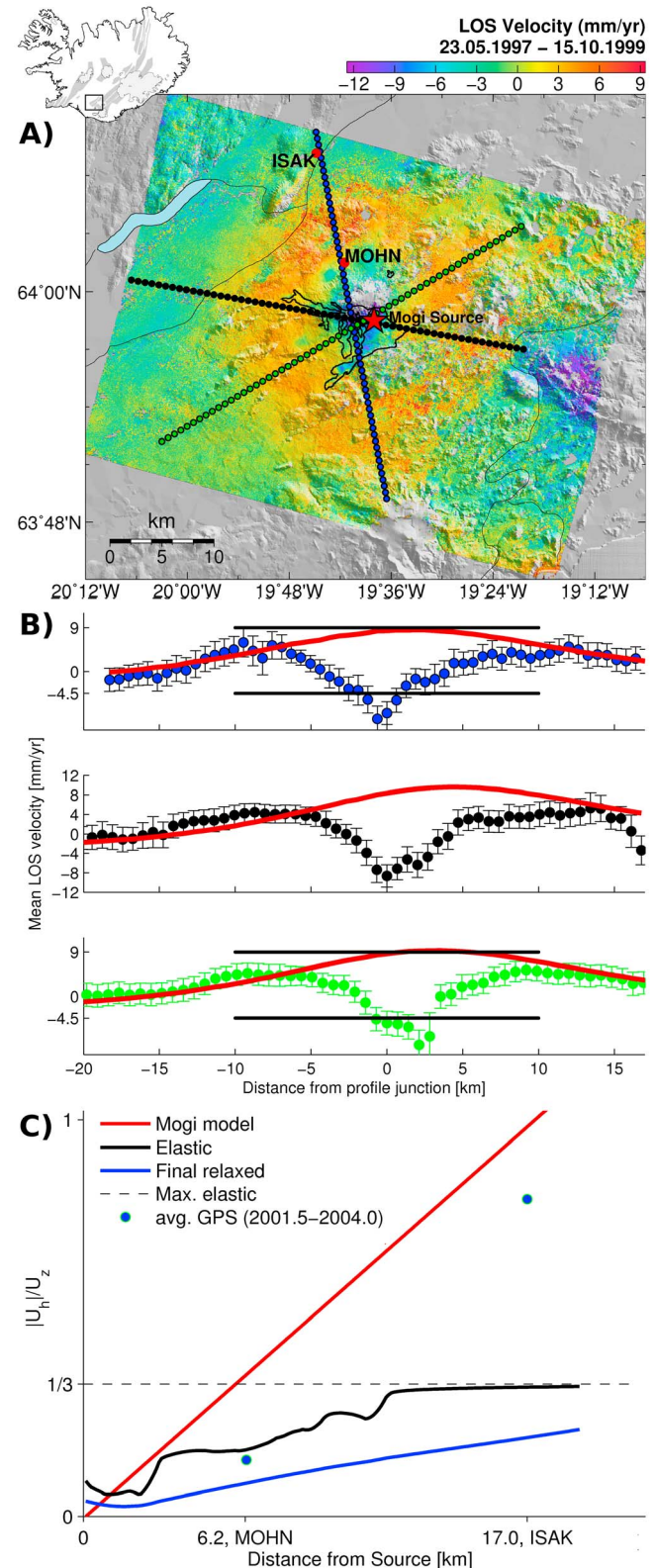
[10] We now invert the superposed signal first for a Mogi source and then for a sill. We search the gridded model space (cell size [length \times width \times depth] = $500 \times 500 \times 100 \text{ m}$) for a pressure source that fits the composite data best in a root-mean-square error (RMSE) sense. The Mogi source with the smallest RMSE is located at depth $d = 8.8 \text{ km}$ with a volume of $V = -0.15 \text{ km}^3$; clearly deeper and about 6 times more voluminous than the original source (Figure 1a; fitted source is light gray). The best fitting sill is found at depth $d = 14.8 \text{ km}$ with length and width of 4.5 km , and opening of 3 m . The volume $V = -0.061 \text{ km}^3$ of this sill is about 2.4 times that of the original source (Figure 1a; fitted sill is black). This case of loading and deflation results in constructive interference of the deformation signals. Inverting these data for a single buried deformation source yields a deeper, more voluminous magma reservoir. Similar overestimates originate from the opposite case of unloading and inflation. Destructive interference can be quite obvious in the data as a pattern of alternating uplift and subsidence is expected to emerge (Figure 2a). Depending on signal strengths, however, this alternation may be subtle, or even disregarded when spatial sampling is sparse. Inverting a signal of destructive interference for a single buried deformation source results in a shallower, less voluminous magma reservoir.

[11] Figure 1a shows the displacements for the best fitting Mogi and sill source as light gray and black dash-dotted lines, respectively. Most of the misfit is found in the horizontal displacement field resulting from the small horizontal deformation contributed by the disk load. In this synthetic example the RMSE of the sill (9.27 mm) is slightly smaller

than that of the Mogi source (9.84 mm) which could lead to a preference for the wrong source geometry.

[12] Figure 1b shows the respective displacement ratios of the data presented in Figure 1a over distances up to 30 km away from the center of the source where the displacements converge to zero. The ratio of the superposed data (green) is clearly distinct from the ratios of forward and inverse

Figure 2. (a) Mean line of sight (LOS) velocity from 23.05.1997–15.10.1999 at Hekla. Circles mark profiles shown in Figure 2b. Black outline in center marks 1991 lava, note subsidence signal (see text). (b) Dots show LOS velocity for the respective profiles in Figure 2a, averaged over number of covered coherent pixels. Red line indicates expected LOS velocity without load effects due to a Mogi source inferred from InSAR data (volume = $0.01 \text{ km}^3 \text{ yr}^{-1}$, depth = 17.2 km (Ófeigsson et al., submitted manuscript, 2010). Horizontal bars mark LOS velocity of -13.5 mm yr^{-1} that is inferred to be due to surface loads and needs to be removed from the data. (c) Displacement ratios for the hypothetical Mogi source (red), surface load due to lavas from 1947–1991 (black: elastic, blue: final relaxed), maximum ratio for any elastic response, and averaged GPS ratios for station MOHN and ISAK. The difference between Mogi model and GPS ratio suggests that the data are affected by additional processes such as adjustments to surface load changes.



models. It first follows the ratio for the best fitting Mogi source and then parallels the disk load ratio. Except for a small perimeter around the source it also exceeds $\frac{1}{3}$ which is atypical for load signals. In addition, this ratio is non-linear which we would not expect for a pressure source. This analysis of the ratio gives sufficient evidence to conclude that a pressure source alone cannot explain the displacement data and additional effects need to be considered.

4. Quantification and Removal of Surface Load Effects

[13] To derive a method for removal of a load signal we now consider the deformation of Hekla volcano in south Iceland (Figure 2a). The average line of sight (LOS) deformation at Hekla from 23.05.1997 to 15.10.1999 has been inferred from InSAR data as described by B. G. Ófeigsson et al. (Deep magma storage at Hekla volcano, Iceland, based on InSAR time series analysis, submitted to *Journal of Geophysical Research*, 2010). Three distinct deformation sources are seen in Figure 2a: a circular uplift around Hekla, subsidence in the center of this circular feature, and subsidence to the ESE of Hekla related to processes at Torfajökull volcano. Here we focus on the central subsidence and uplift feature.

[14] We relate the uplift pattern to inflation of a deep spherical source at ≥ 10 km depth connected to the surface through a shallow dike that was active during the co-eruptive period [Sturkell et al., 2005]. Recharge of the system is modeled as an inflating Mogi source. The central subsidence shows both a circular and an irregular deformation pattern. The latter correlates well with the lava from an eruption in 1991 (black outline in Figure 2a). This signal is likely induced by contraction cooling of the lava or the shallow dike [e.g., Sigmundsson et al., 1997], shallow viscoelastic effects [e.g., Briole et al., 1997], or a combination of these. The circular subsidence, however, reaches beyond recent lava flow edges and we seek to explain it by a viscous response due to loading with lava flows.

[15] To estimate this loading signal we first create profiles of averaged LOS displacements (Figures 2a and 2b). Along these we calculate inflation rates due to an approximated Mogi source (red lines Figure 2b). Ófeigsson et al. (submitted manuscript, 2010) masked out prominent subsidence features prior to the inversion to minimize load effects on depth and volume estimates of 17.2 km and $0.01 \text{ km}^3 \text{ yr}^{-1}$, respectively. The difference of about -13.5 mm yr^{-1} in maximum Mogi source LOS velocity and the profile data outside the 1991 lava flow now serves as a conservative estimate for the surface load contribution to the velocity field. We compare the displacement ratios for the Mogi source (red) to average displacements at the GPS sites MOHN and ISAK (dots) from 2001.5 to 2004 [Sturkell et al., 2005] in Figure 2c. The GPS ratios support the assumption of a composite deformation signal since they are too low to be consistent with the predictions of the Mogi model inferred from masked InSAR data. Although the GPS data are more recent than the InSAR data (1997–1999), their use is legitimate since observations indicate a similar process during pre-eruptive periods (e.g., Ófeigsson et al., submitted manuscript, 2010).

[16] In order to remove the load bias from the velocity field we have to model the contribution of lava flows likely

to affect deformation during the observation period. Considering the relatively low regional viscosity for the upper mantle underneath Iceland inferred by, e.g., Pagli et al. [2007], we assume a quick isostatic adjustment to load changes at Hekla and include lavas erupted since 1947 in our model (average thicknesses in parentheses inferred from volumes [e.g., Höskuldsson et al., 2007] and lava areas): 1947 (34.6 m), 1970 (9.5 m), 1980 (4.0 m), 1981 (3.8 m), 1991 (5.3 m). Our method uses the CrusDe modeling code [Grapenthin, 2007] which implements Green's functions to infer the crustal response to load changes. This requires a priori information on the Earth's structure. Specifically, we need information about the Young's modulus, Poisson's ratio, elastic plate thickness, and effective relaxation time. We expect one or more of these parameters to be unknown for most places. The following recipe for the Hekla example describes how to fix some of these parameters prior to load removal.

[17] We assume a Poisson's ratio $\nu = 0.25$ and a viscous fluid density $\rho_f = 3100 \text{ kg m}^{-3}$. The effective Young's modulus, $E = 40 \text{ GPa}$, can be derived from the study of seasonal signals in regional continuous GPS data as demonstrated by Grapenthin et al. [2006]. Given these values we can now estimate the elastic plate thickness, H , which controls the width of the response. We fit the width of the subsidence feature in Figure 2a which is about 15–20 km by calculating the final relaxed responses due to all lava loads for a range of elastic plate thicknesses and find a best fit for $H = 3.5 \text{ km}$.

[18] With a fixed elastic plate thickness we can now estimate the effective relaxation time, t_r , which controls the duration of the transition from elastic to final relaxed response. The relationship given by Pinel et al. [2007, equation 17] allows us to model the response to the load history of Hekla over a range of values for this parameter. We can approximate the difference of about -13.5 mm yr^{-1} in LOS velocity observed for the year 1999 with $t_r = 100 \text{ yr}$. This corresponds to an effective viscosity of $\eta = 1.2 - 2.4 \times 10^{17} \text{ Pa s}$ assuming a load wavelength of 16–32 km, respectively [Turcotte and Schubert, 2002, equation 6–105]. The cumulative effect of the lava flows is found by adding up the individual responses which are determined using a map of the lava flows, their thicknesses and the time of emplacement. The load induced deformation signal can now be removed from the velocity field (e.g., Ófeigsson et al., submitted manuscript, 2010).

5. Discussion and Conclusions

[19] We demonstrated the effect of surface loads on the inferred parameters of a hypothetical spherical magma reservoir and how to quantify and remove such a load signal from deformation data. Since the displacement ratio for surface loads has a significantly different character from buried magmatic sources we expect similar results for other source geometries.

[20] In this study we did not include thermally induced deformation of the young 1991 lava flow. In order to study load effects we concentrated on deformation outside the lava fields. The estimation of the displacement rates imposed by the surface loads at Hekla is biased in that we have to assume a hypothetical Mogi source at first to get this value. We consider the resulting error for the effective

relaxation time negligible compared to the error in the source estimates. Future work, however, should apply our method in places where the respective crustal parameters have already been determined which would allow for a rigorous error analysis.

[21] Our derived estimates for elastic plate thickness $H = 3.5$ km and effective relaxation time $t_r = 100$ yr, and hence an effective viscosity of $3 - 6 \times 10^{17}$ Pa s, compare well to previous studies [LaFemina et al., 2005; Pinel et al., 2007]. The value of the viscosity, however, may seem underestimated compared to values of $4 - 10 \times 10^{18}$ Pa s, derived for the upper mantle underneath the nearby Vatnajökull ice cap [Pagli et al., 2007]. This difference may reflect the fact that our study region is small and consists of one volcanic center in the young Eastern Rift Zone whereas Pagli et al. [2007] integrate effects over a larger area that extends farther away from the Rift Zone.

[22] We conclude that the gradual viscous response to lava loads emplaced over periods of decades to centuries induces a deformation signal that should be considered for magma source inversions in volcanic areas with high lava production. For uncorrected deformation data, constructive load and pressure source interference may result in an overestimate of depth and volume of a magma reservoir. Destructive signal interference, however, may cause the source parameters to be underestimated. In both cases the source geometry preference could be biased. We find that the ratio of displacements aids the identification of composite signals and suggest to apply this tool more rigorously to deformation data. Once recognized, lava load signals can be quantified and removed. A byproduct of the presented method are values for the elastic thickness of the crust and the effective viscosity beneath the elastic crust.

[23] **Acknowledgments.** Grants from the Icelandic Research Fund and the University of Iceland Research Fund are acknowledged. RG was supported by NSF award EAR-0409950 and the Alaska Volcano Observatory, and thanks Jeff Freymueller for valuable comments on the manuscript. Comments by an anonymous reviewer improved the manuscript.

References

- Bonafede, M., and C. Ferrari (2009), Analytical models of deformation and residual gravity changes due to a Mogi source in a viscoelastic medium, *Tectonophysics*, *471*, 4–13, doi:10.1016/j.tecto.2008.10.006.
- Briole, P., D. Massonnet, and C. Delacourt (1997), Post-eruptive deformation associated with the 1986–87 and 1989 lava flows of Etna detected by radar interferometry, *Geophys. Res. Lett.*, *24*, 37–40.
- Grapenthin, R. (2007), CrusDe: A plug-in based simulation framework for composable CRUSTal DEformation simulations using Green's functions, M.S. thesis, Humboldt Universität zu Berlin, Germany.
- Grapenthin, R., F. Sigmundsson, H. Geirsson, T. Árnadóttir, and V. Pinel (2006), Icelandic rhythmic: Annual modulation of land elevation and plate spreading by snow load, *Geophys. Res. Lett.*, *33*, L24305, doi:10.1029/2006GL028081.
- Heki, K. (2001), Seasonal modulation of interseismic strain buildup in northeastern Japan driven by snow loads, *Science*, *293*, 89–92.
- Höskuldsson, A., N. Óskarsson, R. Pedersen, K. Grönvold, K. Vogfjörð, and R. Ólafsdóttir (2007), The millennium eruption of Hekla in February 2000, *Bull. Volcanol.*, doi:10.1007/s00445-007-0128-3.
- Jull, M., and D. McKenzie (1996), The effect of deglaciation on mantle melting beneath Iceland, *J. Geophys. Res.*, *101*, 21,815–21,828.
- LaFemina, P. C., T. H. Dixon, R. Malservisi, T. Árnadóttir, E. Sturkell, F. Sigmundsson, and P. Einarsson (2005), Geodetic GPS measurements in south Iceland: Strain accumulation and partitioning in a propagating ridge system, *J. Geophys. Res.*, *110*, B11405, doi:10.1029/2005JB003675.
- Lisowski, M. (2007), Analytical volcano deformation source models, in *Volcano Deformation*, chap. 8, pp. 279–304, Springer Praxis, Chichester, U. K.
- Lu, Z., E. Fielding, M. R. Patrick, and C. M. Trautwein (2003), Estimating lava volume by precision combination of multiple baseline spaceborne and airborne interferometric synthetic aperture radar: The 1997 eruption of Okmok Volcano, Alaska, *IEEE Trans. Geosci. Remote Sens.*, *41*(6), 1428–1436.
- Masterlark, T. (2007), Magma intrusion and deformation predictions: Sensitivities to the Mogi assumptions, *J. Geophys. Res.*, *112*, B06419, doi:10.1029/2006JB004860.
- McNutt, S. R., and R. J. Beavan (1987), Eruptions of pavlof volcano and their possible modulation by ocean load and tectonic stresses, *J. Geophys. Res.*, *92*, 11,509–11,523.
- McTigue, D. F., and P. Segall (1988), Displacements and tilts from dip-slip faults and magma chambers beneath irregular surface topography, *Geophys. Res. Lett.*, *15*, 601–604.
- Mogi, K. (1958), Relations between eruptions of various volcanoes and the deformations of the ground surface around them, *Bull. Earthquake Res. Inst. Univ. Tokyo*, *36*, 99–134.
- Okada, Y. (1992), Internal deformation due to shear and tensile faults in a half-space, *Bull. Seis. Soc. Am.*, *82*(2), 1018–1040.
- Pagli, C., and F. Sigmundsson (2008), Will present day glacier retreat increase volcanic activity? Stress induced by recent glacier retreat and its effect on magmatism at the Vatnajökull ice cap, Iceland, *Geophys. Res. Lett.*, *35*, L09304, doi:10.1029/2008GL033510.
- Pagli, C., F. Sigmundsson, B. Lund, E. Sturkell, H. Geirsson, P. Einarsson, T. Árnadóttir, and S. Hreinsdóttir (2007), Glacio-isostatic deformation around the Vatnajökull ice cap, Iceland, induced by recent climate warming: GPS observations and finite element modeling, *J. Geophys. Res.*, *112*, B08405, doi:10.1029/2006JB004421.
- Pinel, V., and C. Jaupart (2005), Some consequences of volcanic edifice destruction for eruption conditions, *J. Volcanol. Geotherm. Res.*, *145*, 68–80.
- Pinel, V., F. Sigmundsson, E. Sturkell, H. Geirsson, P. Einarsson, M. T. Gudmundsson, and T. Högnadóttir (2007), Discriminating volcano deformation due to magma movements and variable surface loads: Application to Katla subglacial volcano, Iceland, *Geophys. J. Int.*, *169*, 325–338.
- Rivalta, E., and P. Segall (2008), Magma compressibility and the missing source for some dike intrusions, *Geophys. Res. Lett.*, *35*, L04306, doi:10.1029/2007GL032521.
- Sigmundsson, F., H. Vadon, and D. Massonnet (1997), Readjustment of the Krafla Spreading Segment to crustal rifting measured by satellite radar interferometry, *Geophys. Res. Lett.*, *24*, 1843–1846.
- Sturkell, E., K. Agustsson, A. T. Linde, S. I. Sacks, P. Einarsson, F. Sigmundsson, H. Geirsson, R. Pedersen, and P. C. LaFemina (2005), Geodetic constraints on the magma chamber of the Hekla volcano, Iceland, *Eos Trans. AGU*, *86*(52), Fall Meet. Suppl., Abstract V21D–0636.
- Turcotte, D. L., and G. Schubert (2002), *Geodynamics*, 528 pp., Cambridge Univ. Press, Cambridge, U. K.
- Williams, C. A., and G. Wadge (2000), An accurate and efficient method for including the effects of topography in three-dimensional elastic models of ground deformation with applications to radar interferometry, *J. Geophys. Res.*, *105*, 8103–8120.
- Wu, P., Z. Ni, and G. Kaufmann (1998), Postglacial rebound with lateral heterogeneities: From 2D to 3D modeling in *Dynamics of the Ice Age*, pp. 557–581, Uetikon, Zurich.

R. Grapenthin, Geophysical Institute, University of Alaska Fairbanks, PO Box 757320, 903 Koyukuk Dr., Fairbanks, AK 99775-7320, USA. (ronni@gi.alaska.edu)

A. Hooper, Delft University of Technology, PO Box 5058, 2600 GB Delft, The Netherlands.

B. G. Ófeigsson and F. Sigmundsson, Nordic Volcanological Center, Institute of Earth Sciences, University of Iceland, Sturlagata 7, 101 Reykjavík, Iceland.

E. Sturkell, Department of Earth Sciences, University of Gothenburg, Box 460, SE-405 30 Gothenburg, Sweden.